Supplementary Information

Simple and General Platform for Highly Adjustable Thermochromic Fluorescent Materials and Multi-Feasible Applications

Jiahui Du,[a] Lan Sheng,*[b] Qiaonan Chen,[a] Yuan Xu,[b] Wen Li,[a] Xiaojun Wang,[a] Minjie Li[a] and Sean Xiao-An Zhang*[a]

[a] State Key Lab of Supramolecular Structure and Materials, College of Chemistry, Jilin University, 130012 Changchun, P. R. China

E-mail: seanzhang@jlu.edu.cn; Fax: +86-431-85153812

[b] College of Chemistry, Jilin University, 130012 Changchun, P. R. China

E-mail: shenglan17@jlu.edu.cn; Fax: +86-431-85153812

Table of contents

Experimental Section

General experimental information

Materials. 4-(Diethylamino)salicylaldehyde (99%), diethyl malonate (99%), POCl3(99.5%), 2,2-Dimethyl-1,3-dioxane-4,6-dione(98%); Hendecanoic acid (HA) (98%), dodecanoic acid (DA) (99%), tetradecanoic acid (TA) (99%), hexadecanoic acid (HcA) (98%), Octadecanoic acid (OA) (98%)were purchased from Energy Chemical (Shanghai, China). Docosanoic acid (DcA) (85%) was purchased from Alfa Aesar (85%) (Shanghai, China). Piperidine (99.5%) was purchased from Aladdin (Shanghai, China). Magnesium chloride ($MgCl_2$•$6H_2O$) were purchased from XiLONG scientific (Shenzhen, China). Llithium chloride (LiCl•H_2O), PEG 20000 (molecular weight: 17,000-22,000) was purchased from Guangfu Fine Chemical Research Institute (Tianjin, China). Potassium carbonate (K_2CO_3•$2H_2O$) was purchased from Sinopharm Chemical Reagent (Beijing, China). Sodium bromide (NaBr•$2H_2O$) was purchased from Tianjin Huadong Reagent (Tianjin, China). Polycaprolactone (PCL) was purchased from Esun (Shenzhen, China). Paraffin wax (PWs) was purchashed from Shanghai Huayong Paraffin co., Ltd. (Shanghai, China) Cellulose filter paper (Whatman-Xinhua, grade 91, Hangzhou, China) was selected as the paper substrate. Unless otherwise noted, all the other materials were purchased from Beijing Chemical Works (Beijing, China) without further purification.

Instruments. Steady state fluorescence spectra were measured using a Shimadzu RF-5301 PC spectrophotometer. The fluorescence quantum yields (Φ_f) and variable temperature fluorescence emission spectra were measured on Edinburgh FLS 920 steady state spectrometer. Fluorescence lifetimes (ns) was measured on Edinburgh FLS 980 using picosecond pulsed diode laser under the excitation at 375 nm. XRD patterns were measured using Empyrean (PANalytical B.V.). Single-crystal X-ray diffraction data was recorded on a Rigaku R-AXIS RAPID diffractometer using the ω-scan mode with graphite monochromator Mo.Kα radiation (λ = 0.71073Å). Differential scanning calorimetry was measured using TA instruments DSC Q20 under pure nitrogen gas with the heating and cooling rates both set to 10 °C min^{-1}. ^1H NMR and ^{13}C NMR were measured on a Bruker AVANCE500 at room temperature. Microscope images were imaged in transmission, reflective and fluorescence modes using Leica DM4000 M microscope. Surface morphologies were characterized using JEOL-6700F filed emission scanning electron microscopy (SEM) at an accelerating voltage of 3KV. Fluorescence images were recorded under UV irradiation at an excitation wavelength of 365 nm.

Preparation of TFMs. Dissolve the coumarins in molten long chain saturated fatty acids (FA) with the assistant of ultrasonic dissolution at the selected optimal concentration (**1**: 3mg, **2**: 1 mg; **3**: 3 mg; **4** – **5**: 2mg) in per gram FA.

Preparation of fluorescent papers. Molecule **1** were dissolved in molten DA (5mg **1** /g DA) and the solutions immersed the filter papers at 60 °C. Excess FA residue was removed by treatment with oil-absorbing paper.

Preparation of coumarin-in-FA pens. A hot solution containing FA (i.e., OA, DcA) and coumarins (**1**: 5mg, **2**: 1 mg; **3**: 5 mg; **4** – **5**: 4 mg in per gram FA, respectively) poured into a mold, cooled to room temperature, and removed from the mold.

Synthesis and characterization

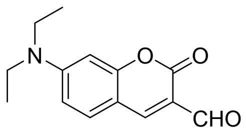

1 was synthesized according to reported literature.[1] ^{1}H NMR (500 MHz, DMSO-d_6): δ 9.90 (s, 1H), 8.41 (s, 1H), 7.68 (d, *J* = 9.1 Hz, 1H), 6.83 (dd, *J* = 9.1, 2.3 Hz, 1H), 6.61 (d, *J* = 2.0 Hz, 1H), 3.51 (q, *J* = 7.0 Hz, 4H), 1.15 (t, *J* = 7.0 Hz, 6H). ^{13}C NMR (125 MHz, DMSO-d_6): δ 187.09, 160.70, 158.44, 153.42, 146.11, 133.05, 113.15, 110.46, 107.67, 96.36, 44.53, 12.34. Melting point: 168.1 ^{o}C.

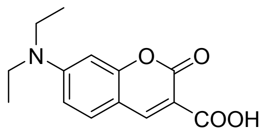

2 was synthesized according to reported literature.[2] ^{1}H NMR (500 MHz, CDCl$_3$): δ 12.34 (s, 1H), 8.66 (s, 1H), 7.46 (d, *J* = 9.0 Hz, 1H), 6.72 (dd, *J* = 9.0, 2.3 Hz, 1H), 6.54 (d, *J* = 2.0 Hz, 1H), 3.50 (q, *J* = 7.1 Hz, 4H), 1.27 (t, *J* = 7.1 Hz, 6H). ^{13}C NMR (125 MHz, CDCl$_3$): δ 165.65, 164.56, 158.16, 153.89, 150.37, 132.07, 111.07, 108.69, 105.69, 96.98, 45.49, 12.51. Melting point: 231 ^{o}C.

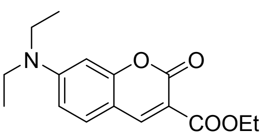

3 was synthesized according to reported literature.[2] ^{1}H NMR (500 MHz, CDCl$_3$): δ 8.42 (s, 1H), 7.36 (d, *J* = 8.9 Hz, 1H), 6.62 (dd, *J* = 8.9, 2.4 Hz, 1H), 6.47 (d, *J* = 2.3 Hz, 1H), 4.37 (q, *J* = 7.1 Hz, 2H), 3.45 (q, *J* = 7.1 Hz, 4H), 1.39 (t, *J* = 7.1 Hz, 3H), 1.23 (t, *J* = 7.1 Hz, 6H). ^{13}C NMR (125 MHz, CDCl$_3$): δ 164.39, 158.58, 158.39, 152.92, 149.30, 131.14, 109.68, 109.21, 107.88, 96.93, 61.28, 45.26, 14.51, 12.54. Melting point: 86.8 ^{o}C.

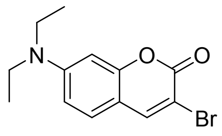

4 was synthesized according to reported literature.[3] ^{1}H NMR (500 MHz, CDCl$_3$): δ 7.90 (s, 1H), 7.23 (d, *J* = 8.9 Hz, 1H), 6.61 (dd, *J* = 8.8, 2.4 Hz, 1H), 6.50 (s, *J* = 2.3 Hz, 1H), 3.43 (q, *J* = 7.1 Hz, 4H), 1.23 (t, *J* = 7.1 Hz, 6H). ^{13}C NMR (125 MHz, CDCl$_3$): δ 158.44, 156.18, 150.93, 144.87, 128.29, 109.43, 109.05, 103.07, 97.47, 45.10, 12.51. Melting point: 138.2 ^{o}C.

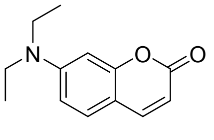

5 was synthesized according to reported literature.[1] ^{1}H NMR (500 MHz, DMSO-d_6): δ 7.82 (d, *J* = 9.3 Hz, 1H), 7.42 (d, *J* = 8.8 Hz, 1H), 6.68 (dd, *J* = 8.8, 2.5 Hz, 1H), 6.51 (d, *J* = 2.4 Hz, 1H), 5.99 (d, *J* = 9.3Hz, 1H), 3.42 (q, *J* = 7.0 Hz, 4H), 1.12 (t, *J* = 7.0 Hz, 6H). ^{13}C NMR (125 MHz, DMSO-d_6): δ 160.99, 156.34, 150.47, 144.47, 129.29, 108.77, 108.17, 107.66, 96.60, 44.02, 12.29. Melting point: 88.6 ^{o}C.

Supplementary Figures

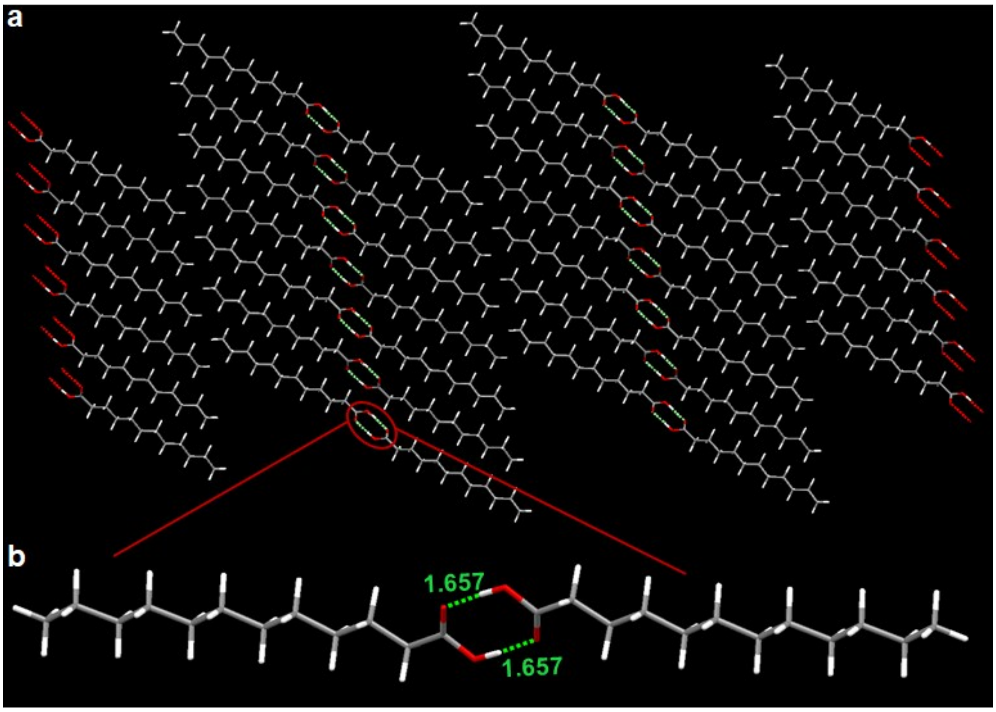

Fig. S1 (a) Single-crystal packing modes of DA. (b) The hydrogen bonding interactions of adjacent molecules. The crystallographic data of DA is acquired from CCDC (deposited number: 738617).

^{1}H NMR and ^{13}C NMR spectra

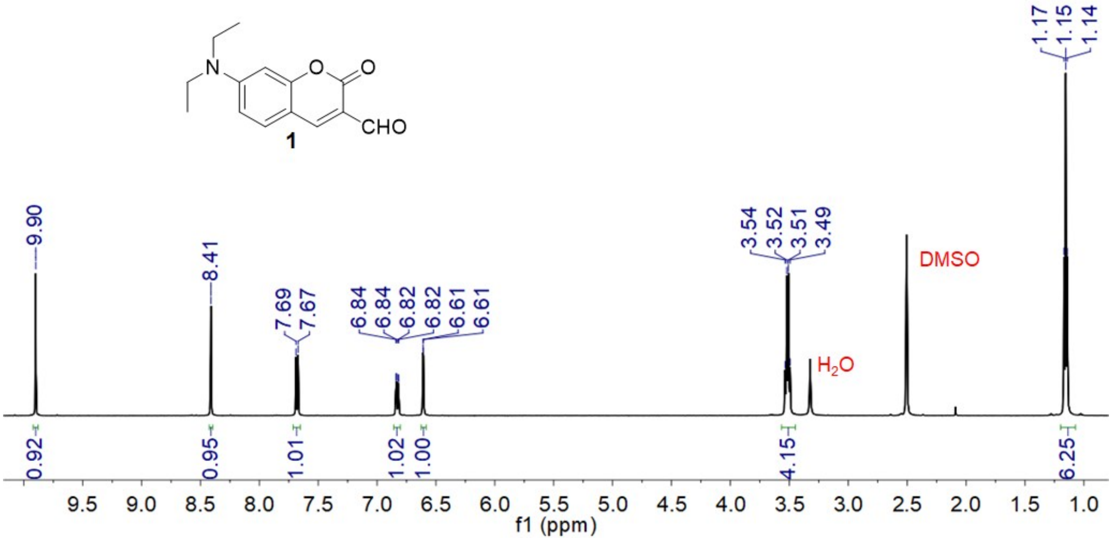

Fig. S2 ^{1}H NMR spectrum of **1** (500 MHz, DMSO-d_6).

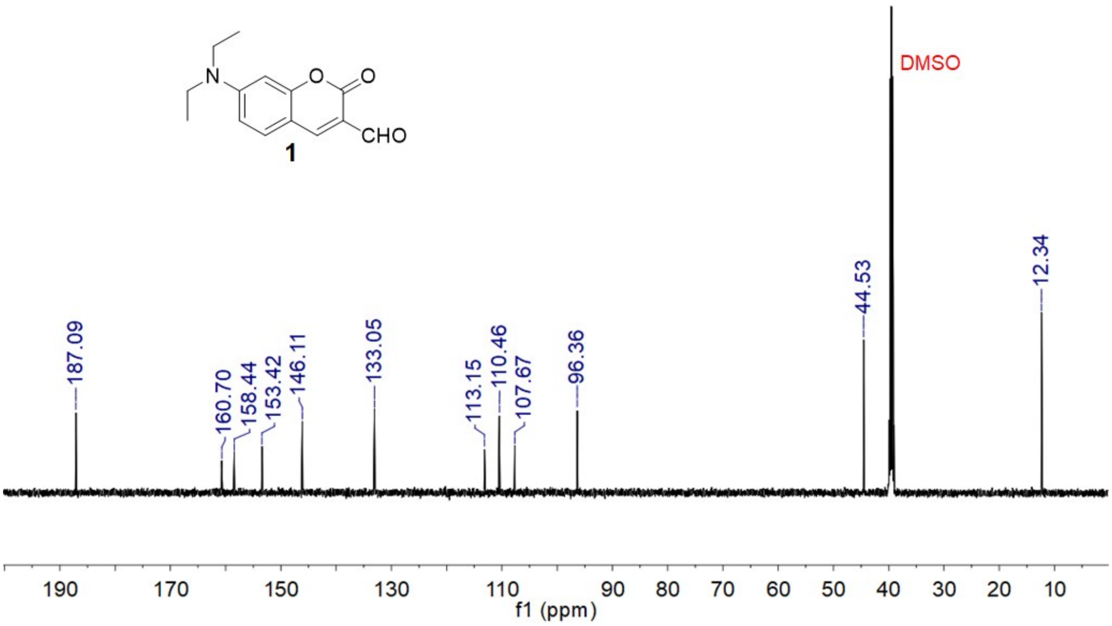

Fig. S3 ^{13}C NMR spectrum of **1** (125 MHz, DMSO-d_6).

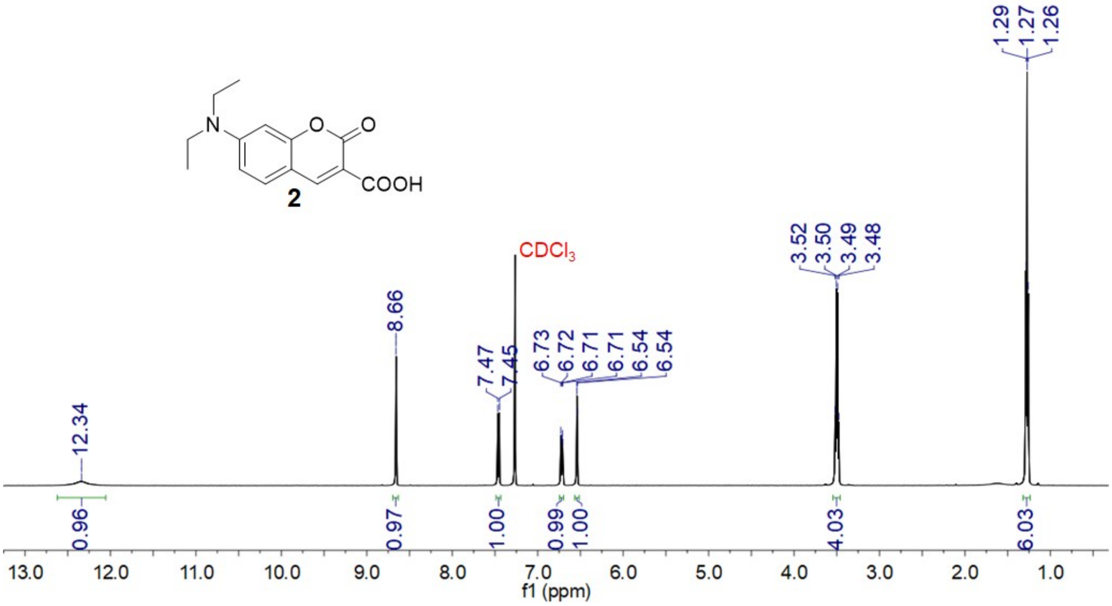

Fig. S4 ^{1}H NMR spectrum of **2** (500 MHz, CDCl$_3$).

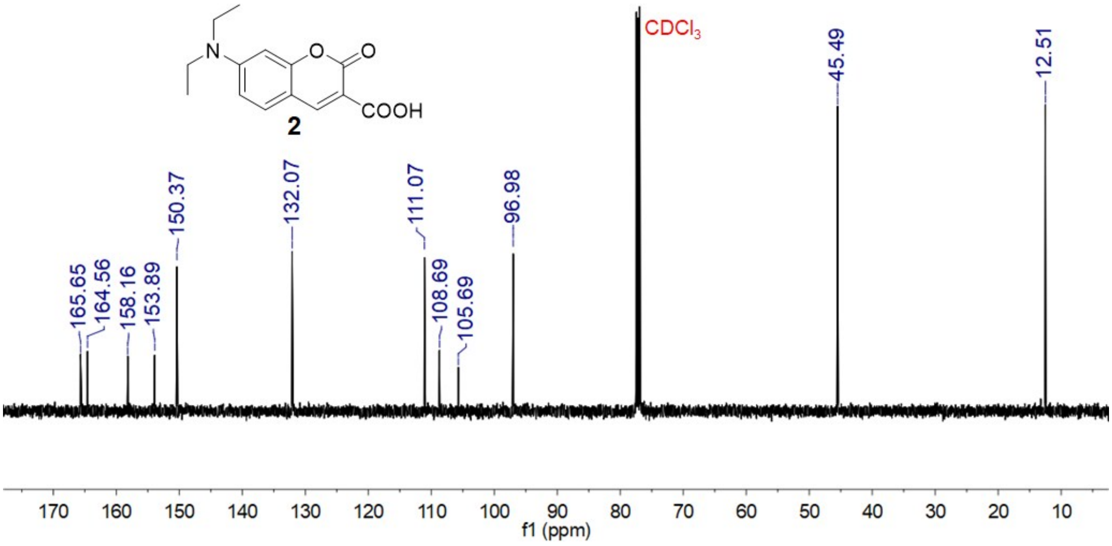

Fig. S5 ^{13}C NMR spectrum of **2** (125 MHz, CDCl$_3$).

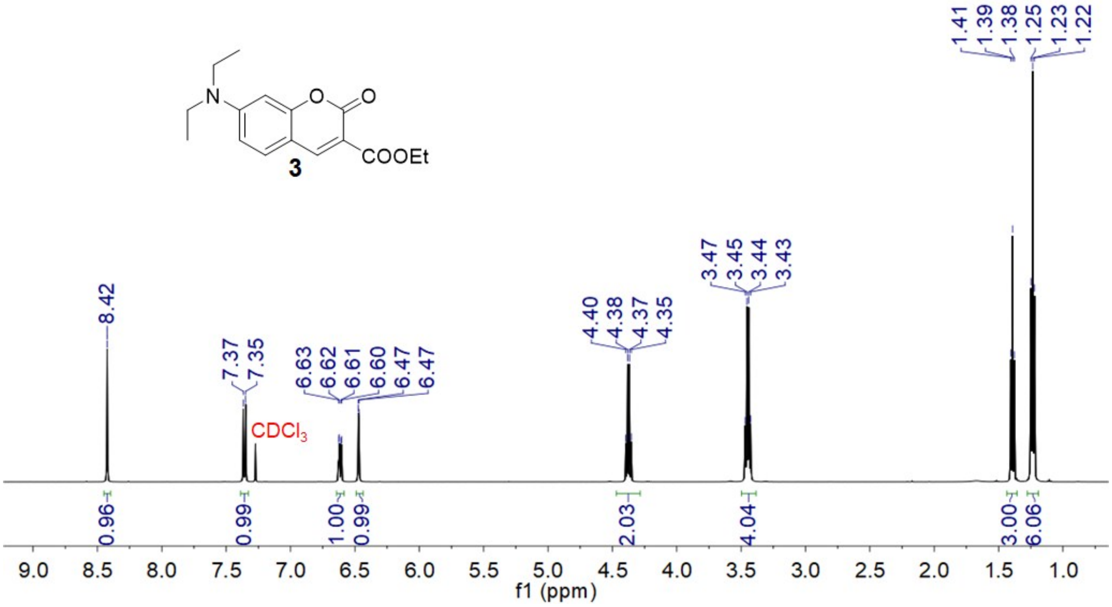

Fig. S6 ^{1}H NMR spectrum of **3** (500 MHz, CDCl$_3$).

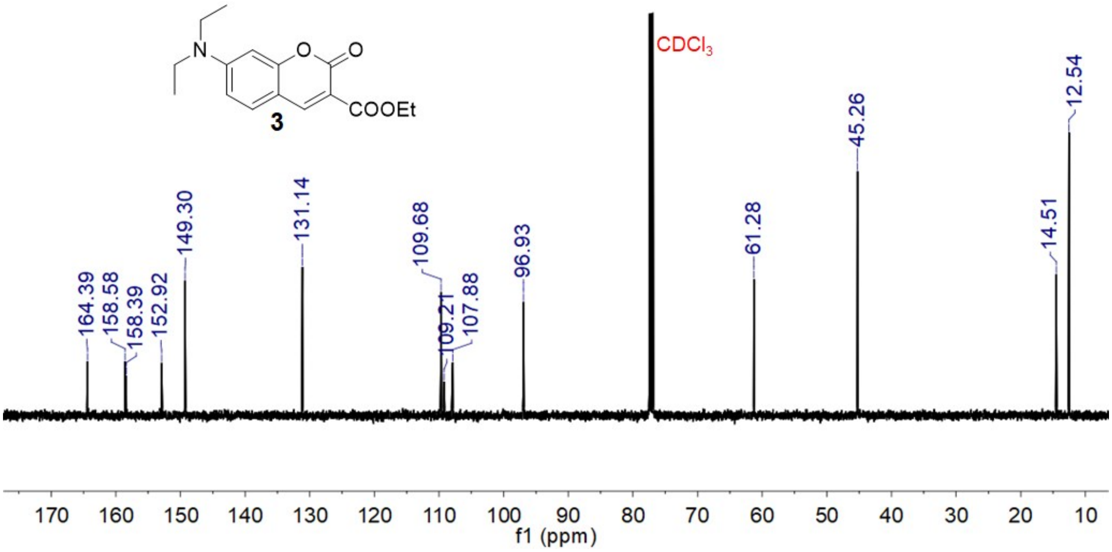

Fig. S7 ^{13}C NMR spectrum of **3** (125 MHz, CDCl$_3$).

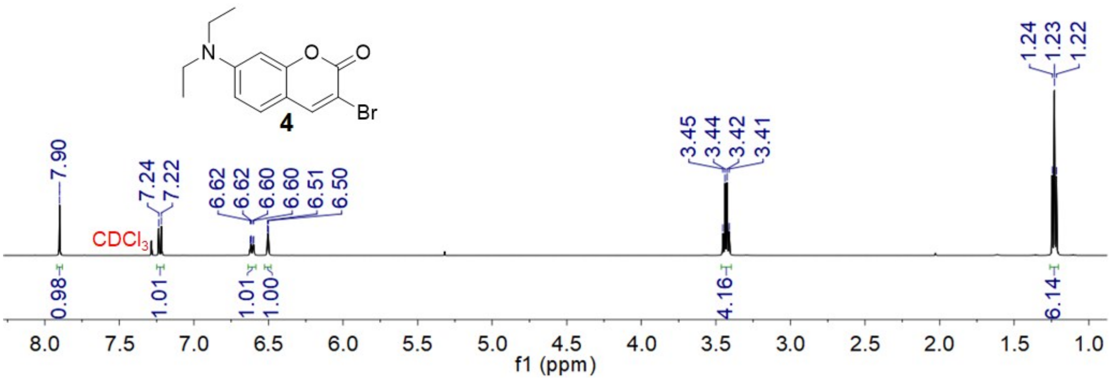

Fig. S8 ^{1}H NMR spectrum of **4** (500 MHz, $CDCl_3$).

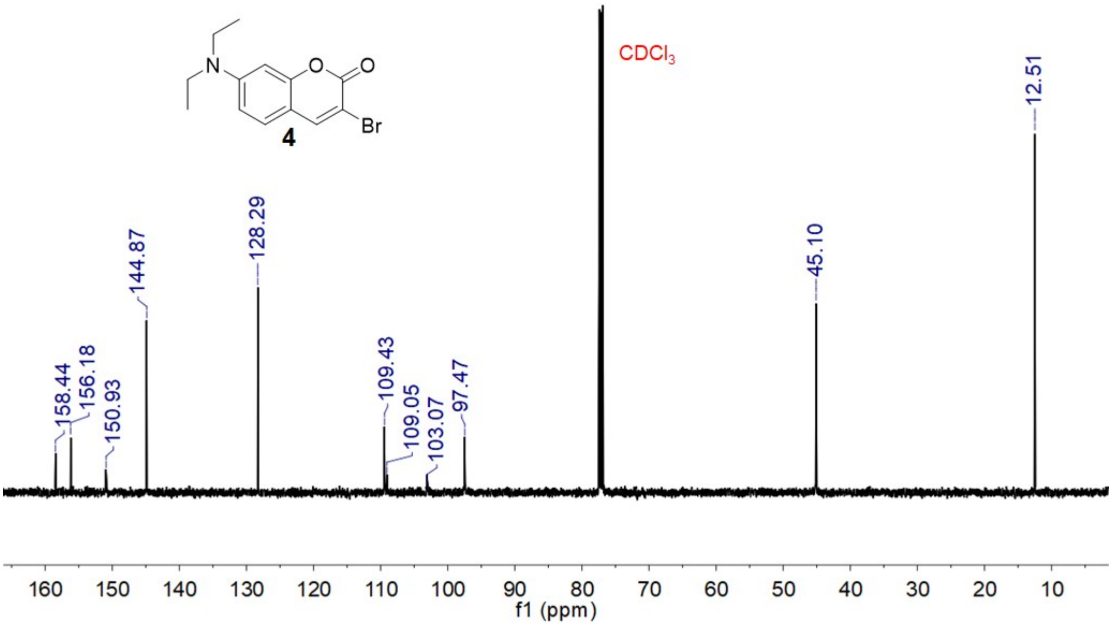

Fig. S9 ^{13}C NMR spectrum of **4** (125 MHz, $CDCl_3$).

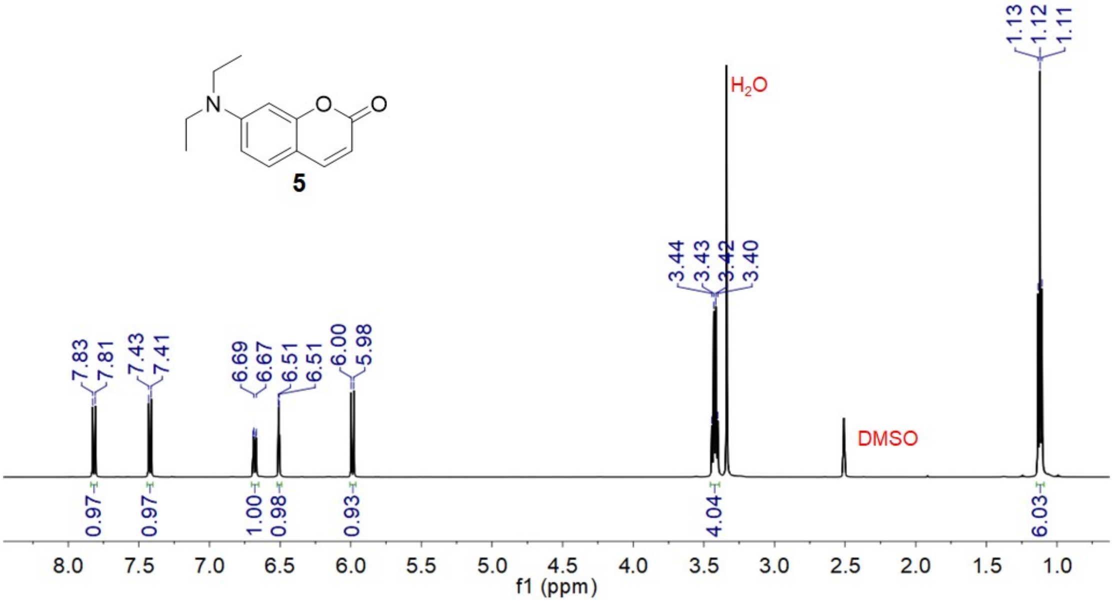

Fig. S10 ^{1}H NMR spectrum of **5** (500 MHz, DMSO).

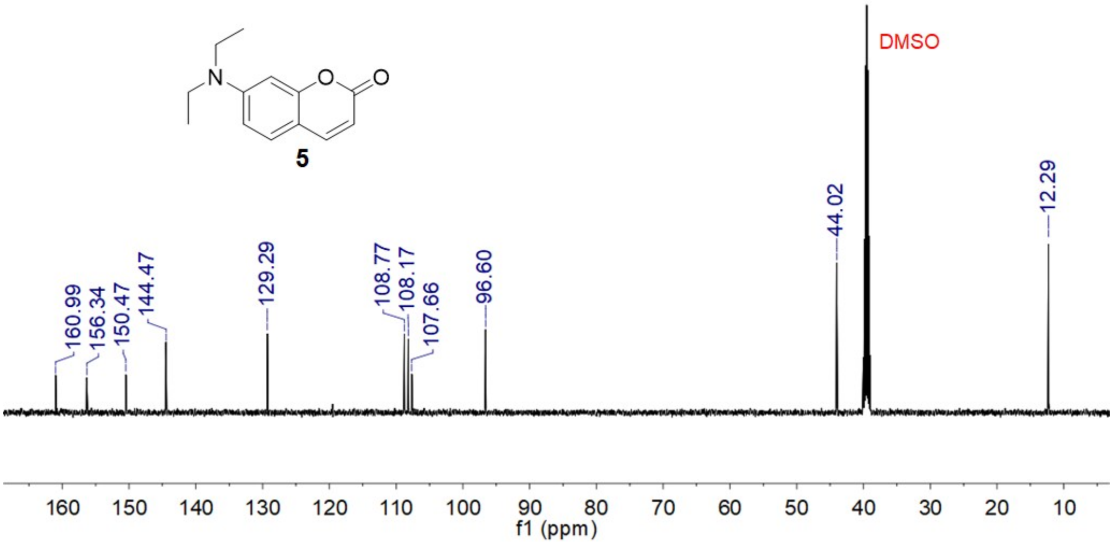

Fig. S11 ^{13}C NMR spectrum of **5** (125 MHz, DMSO).

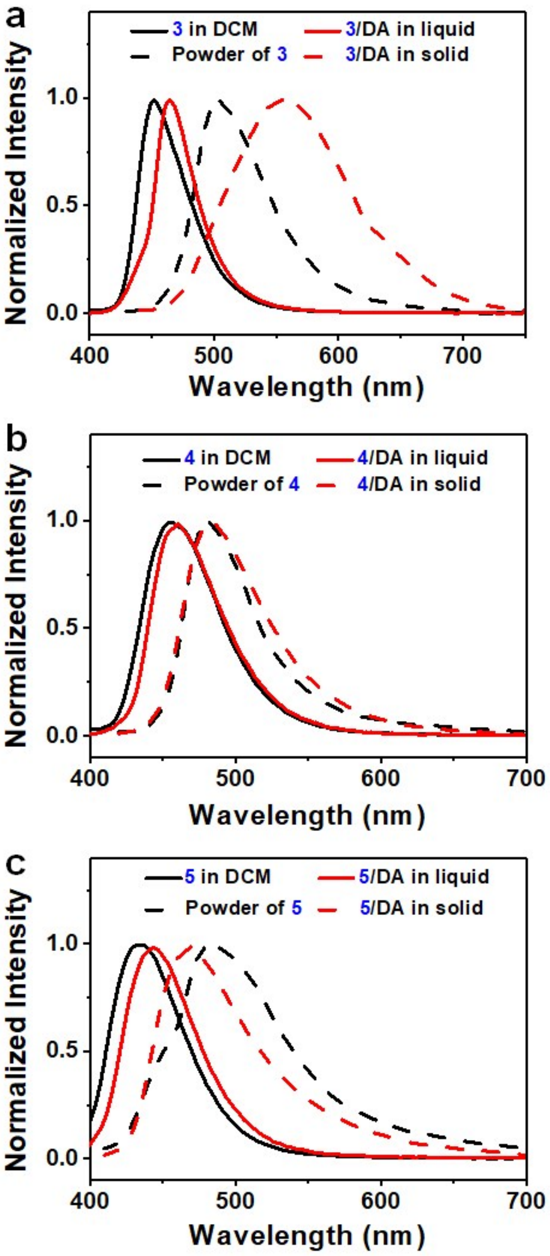

Fig. S12 (a-c) Normalized fluorescence emission spectra of **3** – **5** on their four physical states: powder, in diethylamine (DCM) (C = 1.0 × 10^{-5} mol L^{-1}), and dissolved in dodecanic acid (DA) (0.3 wt%, 0.2 wt%, 0.2 wt%, respectively) in solid and liquid state.

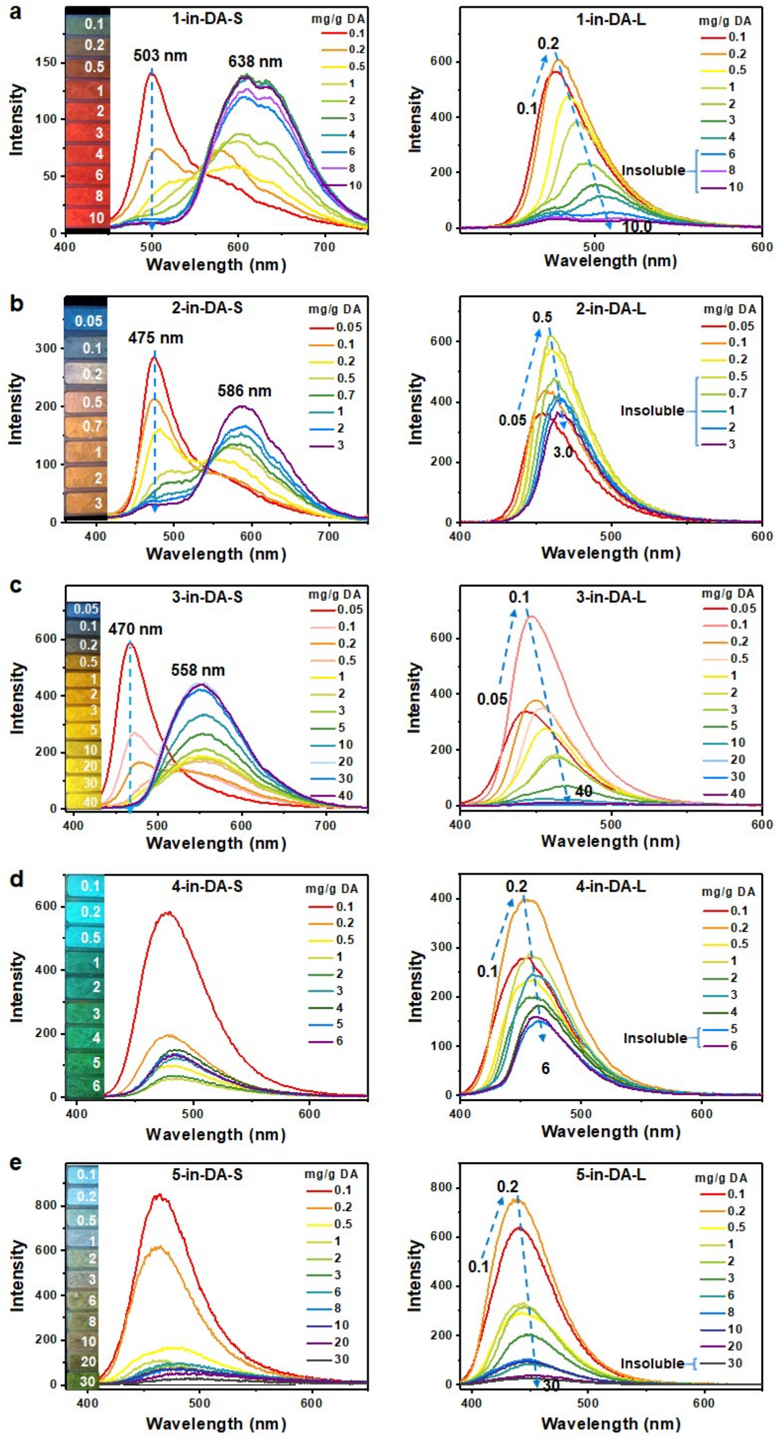

Fig. S13 (a-e) Fluorescence emission spectra of **1** – **5** dissolved in 1 g DA in solid state (left) and liquid state (right) as a function of coumarin concentration. (**1**: λ_{ex} = 400 nm, slit width $(3, 3)_S/(3, 1.5)_L$; **2**: λ_{ex} = 380 nm, $(1.5, 3)_S/(1.5, 1.5)_L$; **3**: λ_{ex} = 400 nm, slit width $(1.5, 3)_S/$ λ_{ex} = 380 nm, slit width $(1.5,1.5)_L$; **4**: λ_{ex} = 400 nm, slit width $(3, 1.5)_S/$ λ_{ex} = 380 nm, slit width $(1.5,1.5)_L$; **5**: λ_{ex} = 380 nm, slit width $(1.5, 3)_S/$ λ_{ex} = 370 nm, slit width $(3,1.5)_L$)

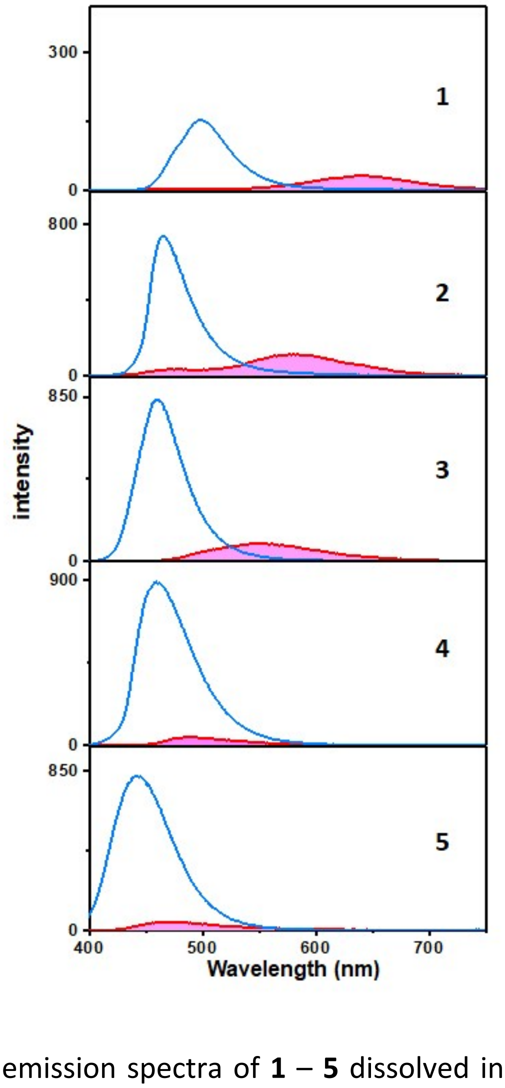

Fig. S14 Fluorescence emission spectra of **1** – **5** dissolved in DA (0.3 wt%, 0.1 wt%, 0.3 wt%, 0.2 wt%, 0.2 wt%) in the solid (red) and liquid (blue) state, respectively. λ_{ex} = 380 nm, slit width (3, 1.5).

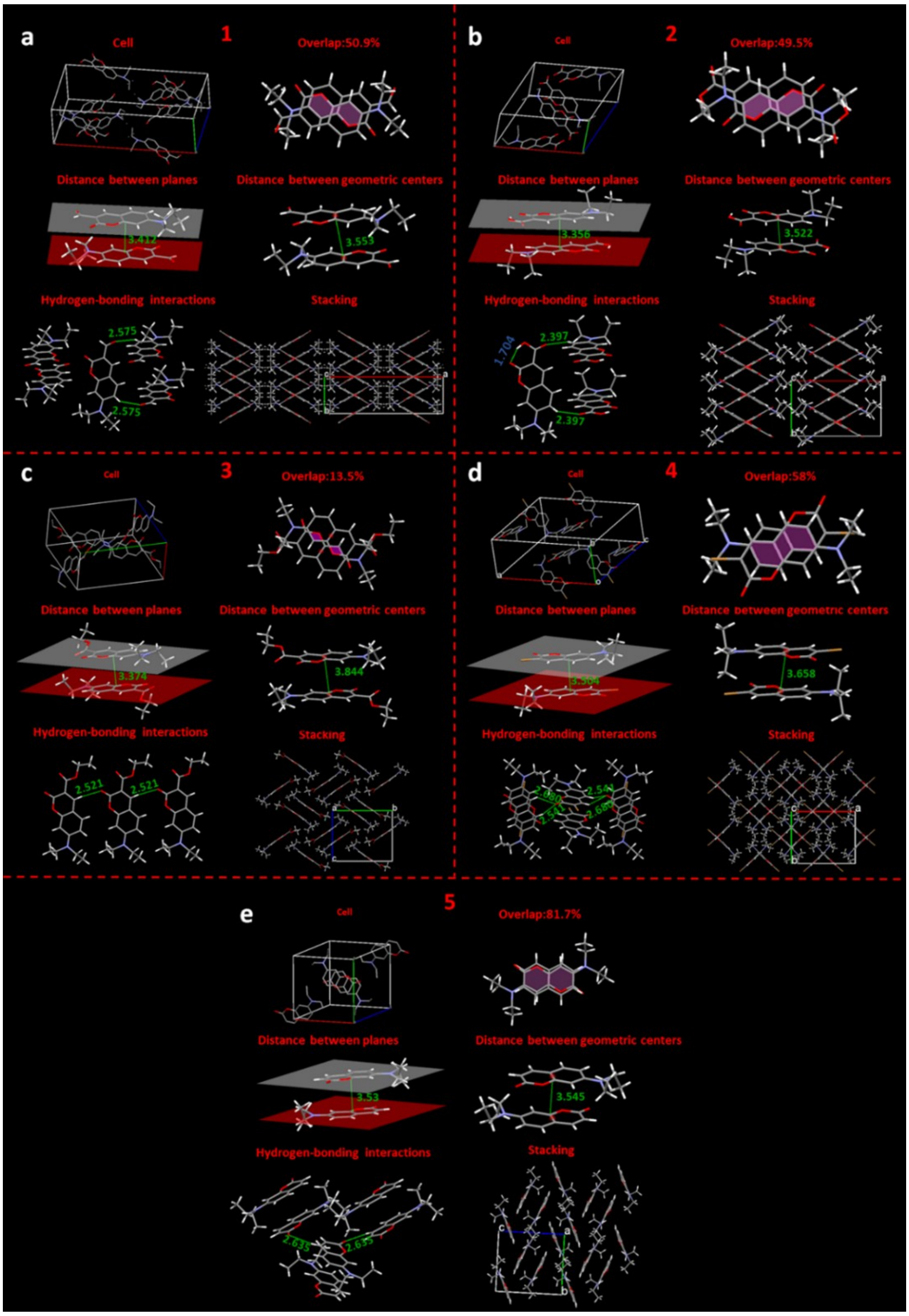

Fig. S15 (a-e) Single crystal structure of **1** – **5**. The single crystal cell, the overlap ratio and distance of two adjacent molecular planes, the distance from the geometric center, the hydrogen bond interaction of adjacent molecules and the entire packing modes of the crystals are listed respectively. The crystallographic data of **1** – **3**, **5** is acquired from CCDC (deposited number: **1**-834384, **2**-613852, **3**-1004829, **4-**1438106, **5-**1459476).

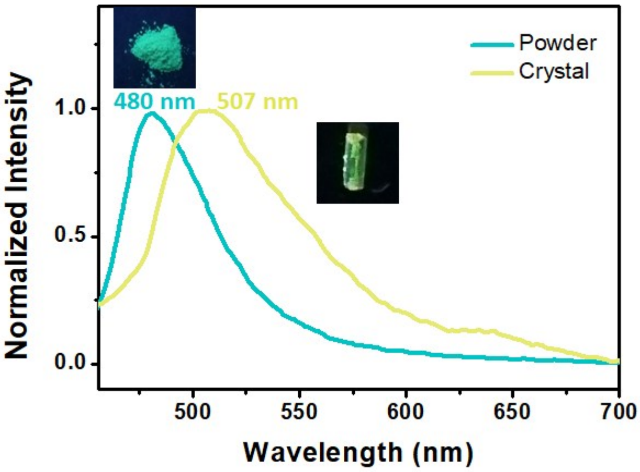

Fig. S16 Normalized fluorescence emission spectra of **4** in powder and crystal state (λ_{ex} = 380 nm).

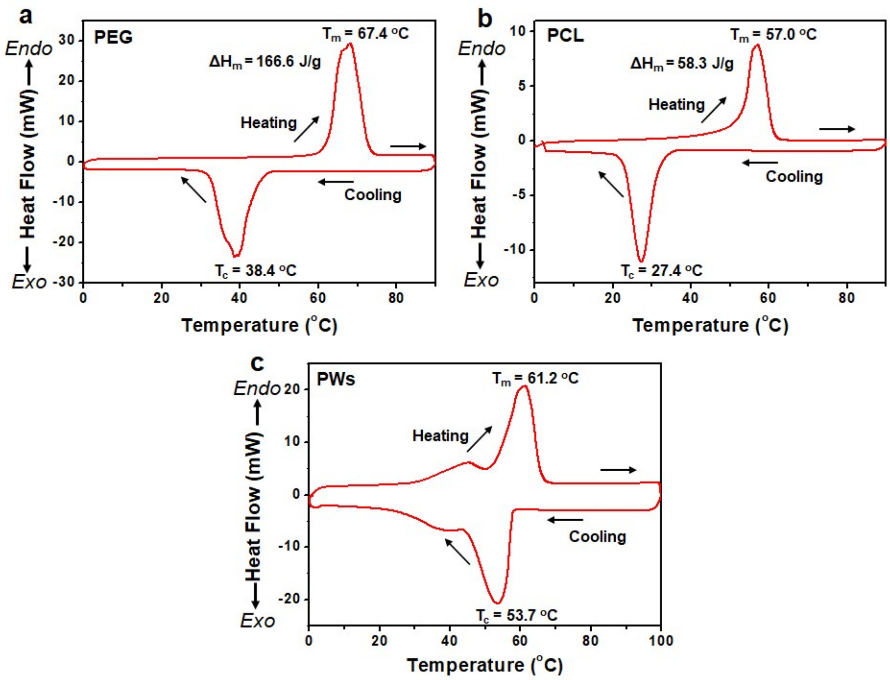

Fig. S17 (a-c) DSC thermograms of poly(ethylene glycol) (PEG), polycaprolactone (PCL) and paraffin waxes (PWs).

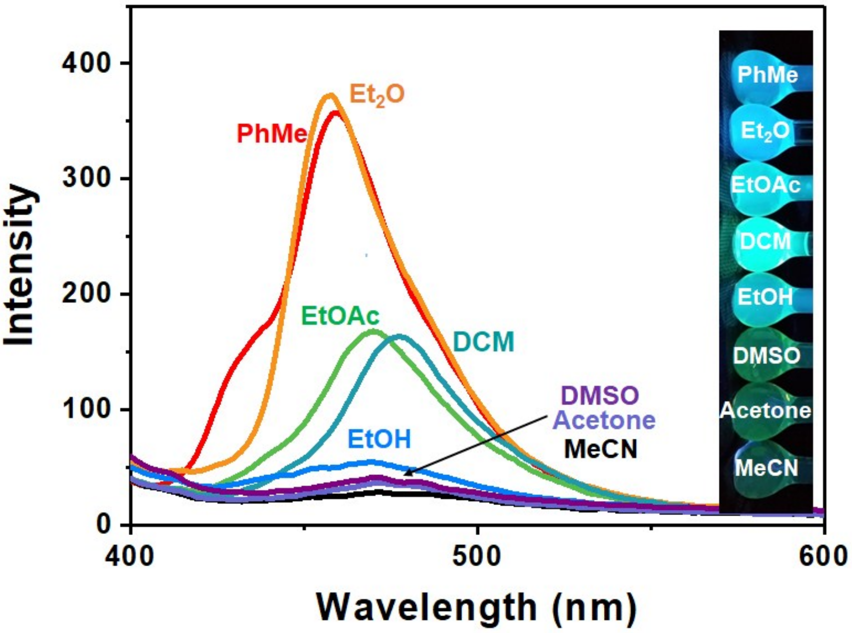

Fig. S18 Fluorescence emission spectra and photographs of **1** in different solvents (C = 1.0×10^{-5} mol L^{-1}), respectively. λ_{ex} = 380 nm, slit width (3, 3).

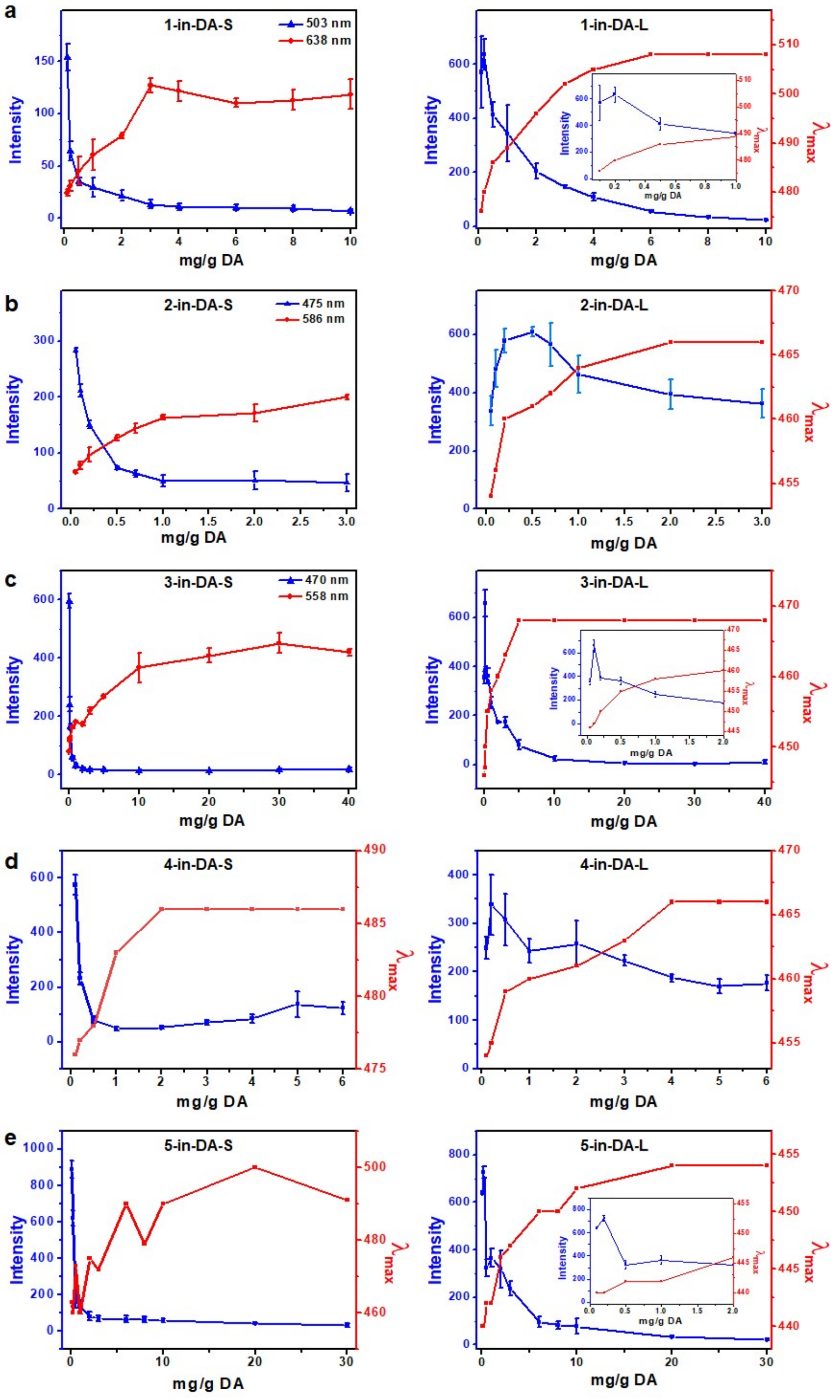

Fig. S19 (a-e) Plots of maximum emission intensity and maximum emission wavelength variation for **1 – 5** with different doped mass in 1g DA in solid (left) and liquid (right) states, respectively.

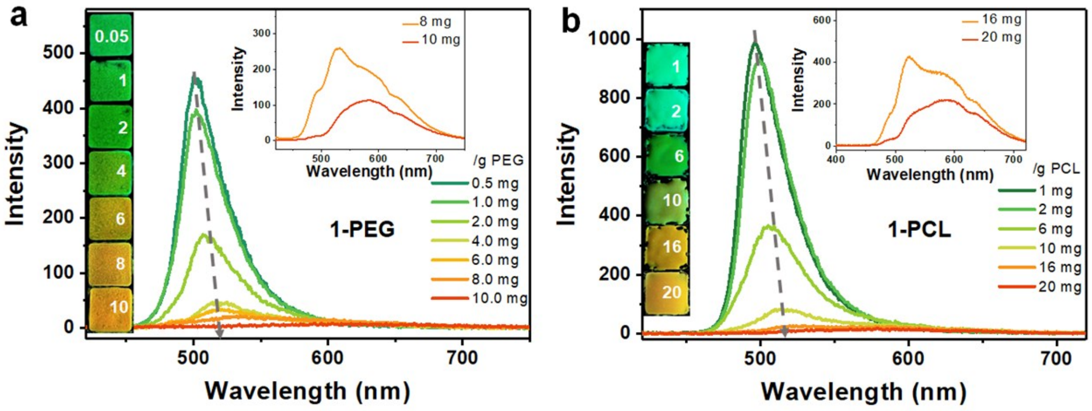

Fig. S20 Fluorescence emission spectra and photographs of **1** dissolved in a) poly (ethylene glycol) (PEG) and b) polycaprolactone (PCL) in solid state with gradually increased concentration. PEG: λ_{ex} = 400 nm, slit width (1.5, 1.5); PCL: λ_{ex} = 385 nm, slit width (1.5, 1.5)

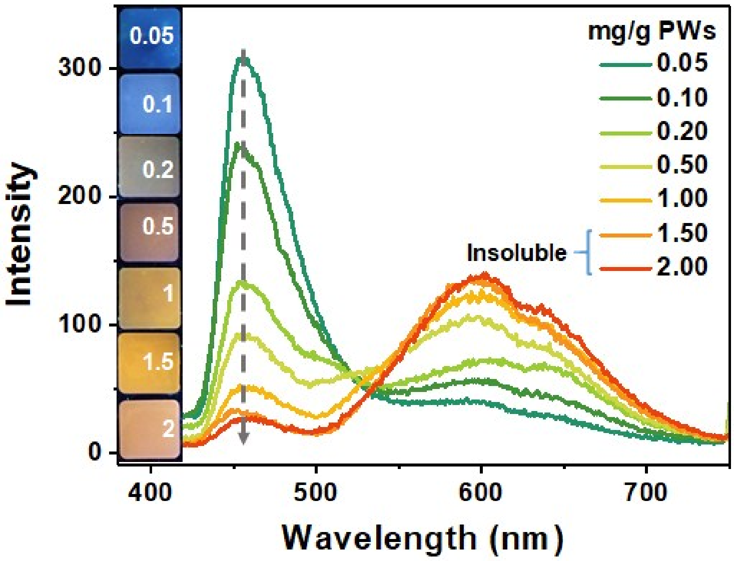

Fig. S21 Fluorescence emission spectra of **1** dissolved in paraffin waxes (PWs) with gradually increased concentration. λ_{ex} = 380 nm, slit width (3, 3).

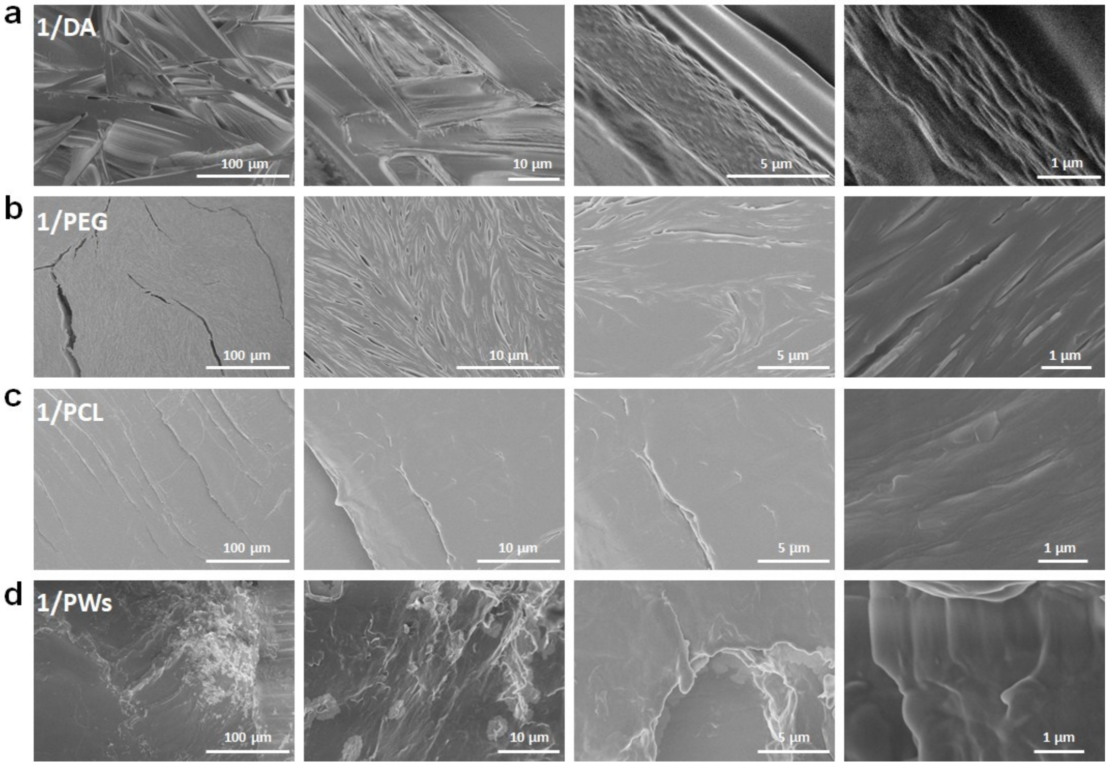

Fig. S22 (a-d) SEM images of **1** in DA, PEG, PCL and PWs under different scales, respectively. (a: 0.3 wt%, b: 1.0 wt%, c: 2.0 wt%, d: 0.1 wt%)

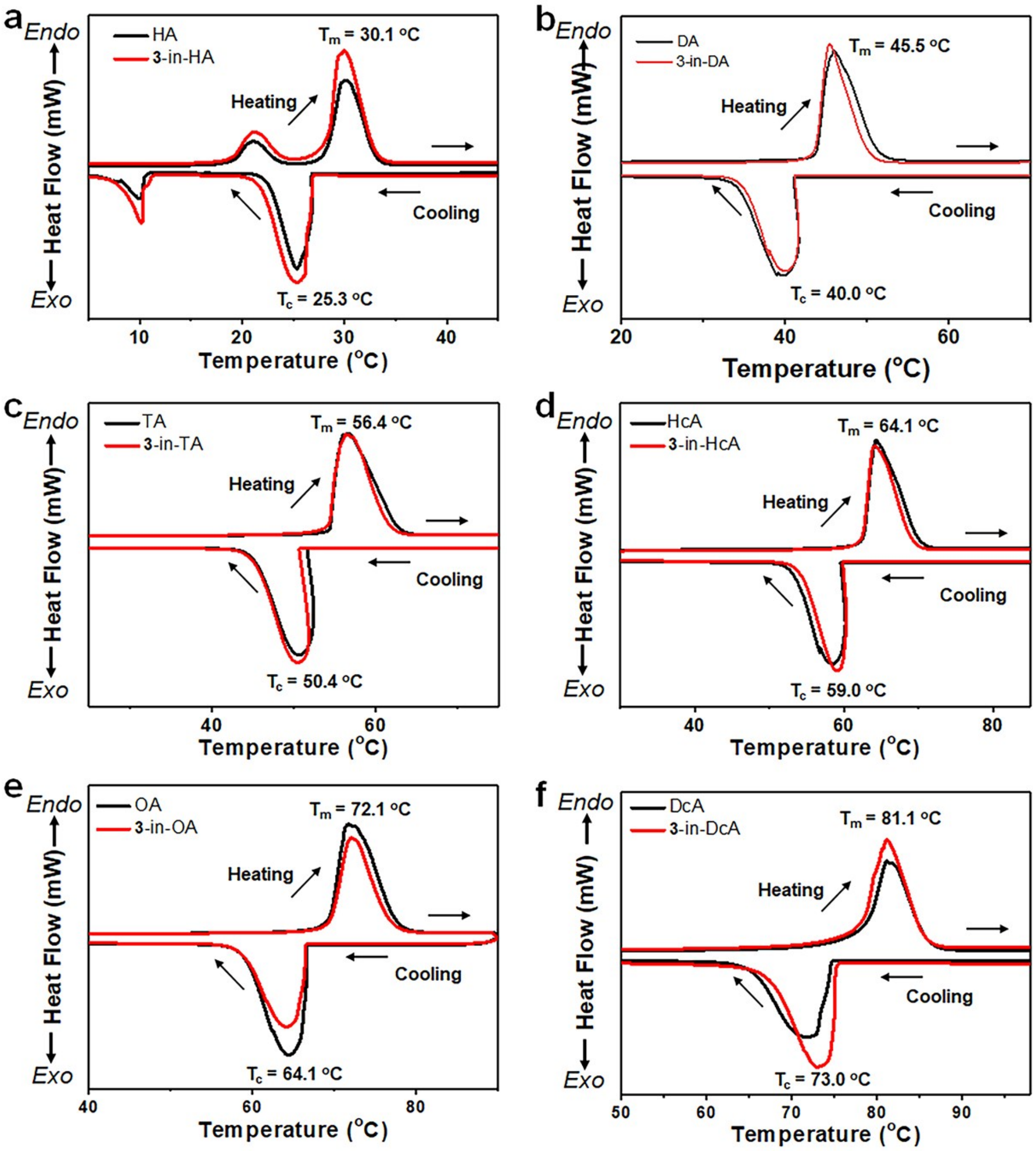

Fig. S23 (a-f) DSC thermograms of pure FA (black line) and **3**-in-FA (red line). The mass ratio of **3** in FA are 0.3 wt%.

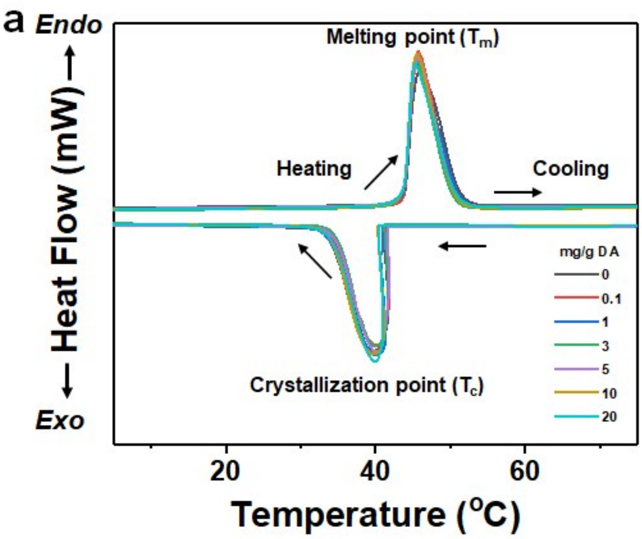

b

mg/g DA	T_m (°C)	T_c (°C)
0	45.9	39.6
0.1	45.7	40.4
1	45.4	40.3
3	45.5	40.0
5	45.7	40.1
10	45.6	40.0
20	45.4	40.0

Fig. S24 Thermodynamic Properties of different doping mass of **3** in 1g of DA.

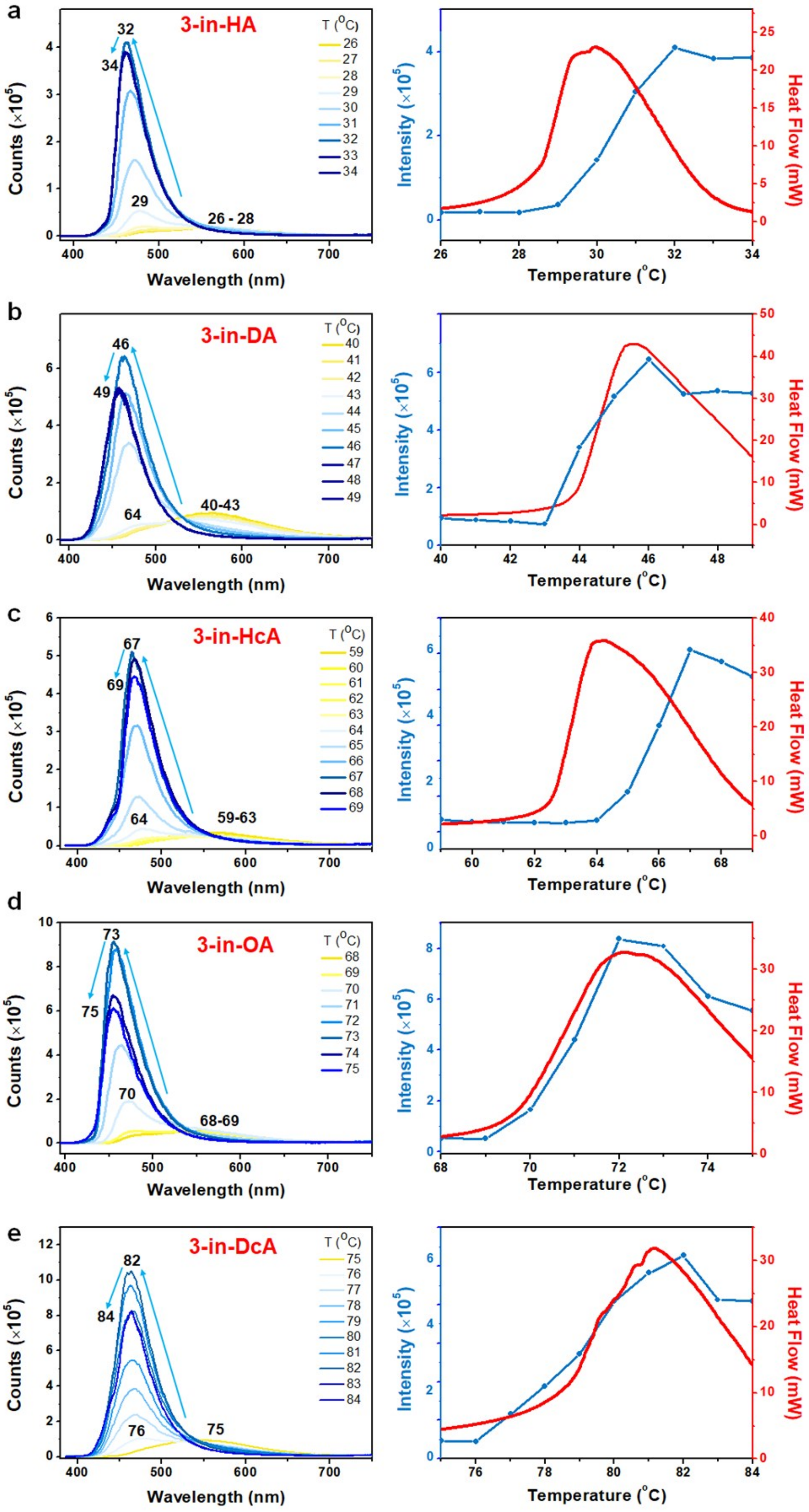

Fig. S25 (a-e) Variable temperature fluorescence spectra (left) and comparative plots of variable of FL intensity and heat flow of **3**-in-FA (0.3 wt %) upon heating (right). (Monitored at the FL maximum wavelength 558 nm (yellow curve, left) and 464 nm (blue curve, left), respectively.)

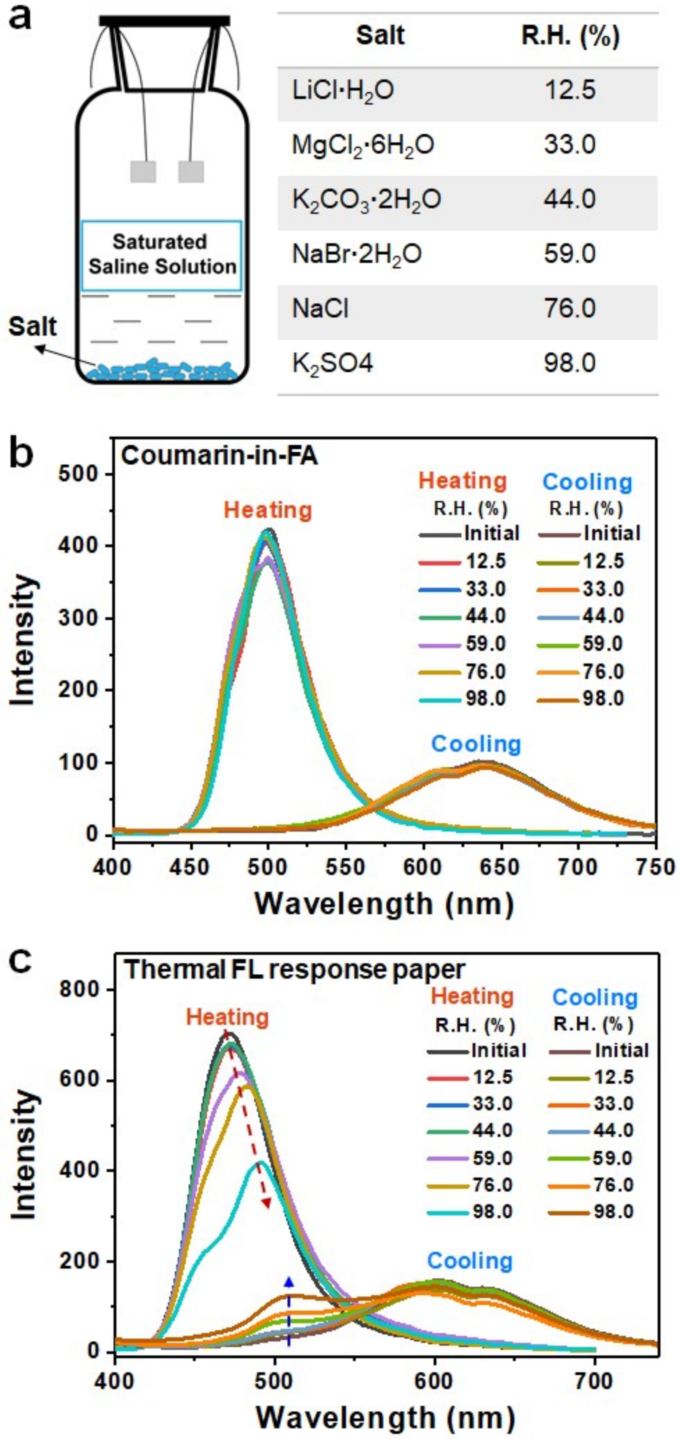

Salt	R.H. (%)
$LiCl\cdot H_2O$	12.5
$MgCl_2\cdot 6H_2O$	33.0
$K_2CO_3\cdot 2H_2O$	44.0
$NaBr\cdot 2H_2O$	59.0
NaCl	76.0
K_2SO4	98.0

Fig. S26 (a) Illustration of the storage of TFMs and thermal response FL papers at different humidity values provided via using different saturated saline solutions referred to standard method^{S4}. (b) Corresponding fluorescence emission spectra for the TFMs after exposed to different humidity ambient 48h. (λ_{ex} = 380 nm, slit width (3, 1.5)). (c) Corresponding fluorescence emission spectra for the thermal response FL papers after exposed to different humidity ambient 12h. Cooling: λ_{ex} = 380 nm, slit width (5, 3); Heating: λex = 400 nm, slit width (3,3).

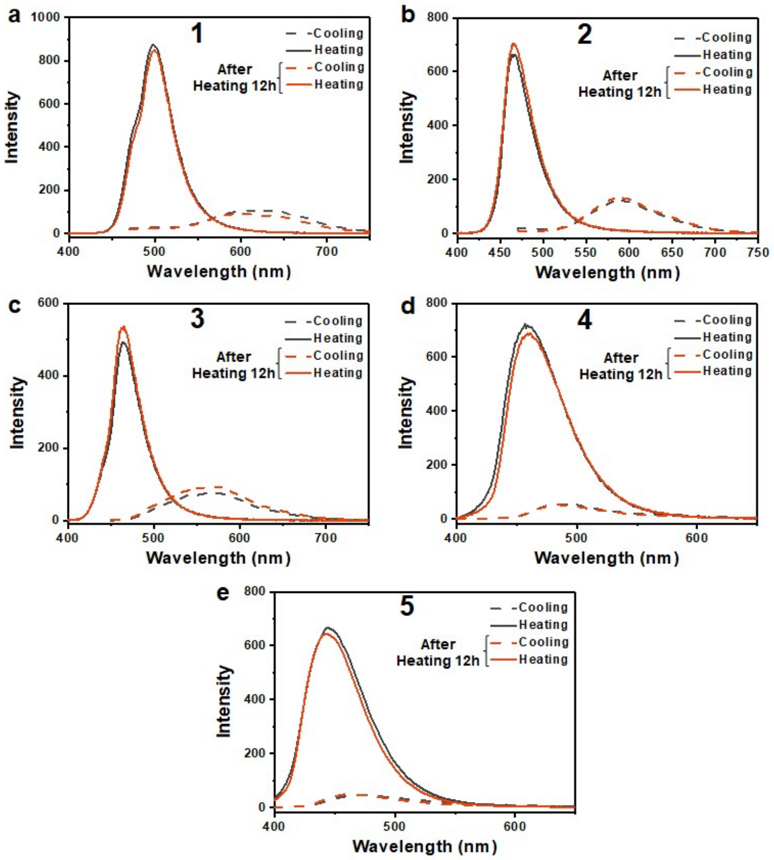

Fig. S27 The comparison of fluorescence emission spectra of **1** – **5** dissolved in DA (0.3 wt%, 0.1 wt%, 0.3 wt%, 0.2 wt%, 0.2 wt%) on the initial state and after heating 12h in 60 ^{o}C water bath.

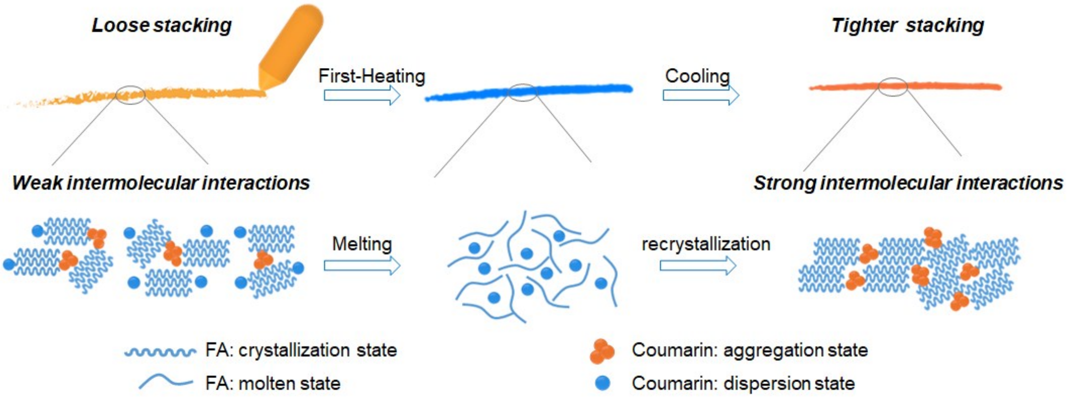

Fig. S28 Schematic illustration describing the first heating and cooling of coumarin-in-OAs drawn on filter paper.

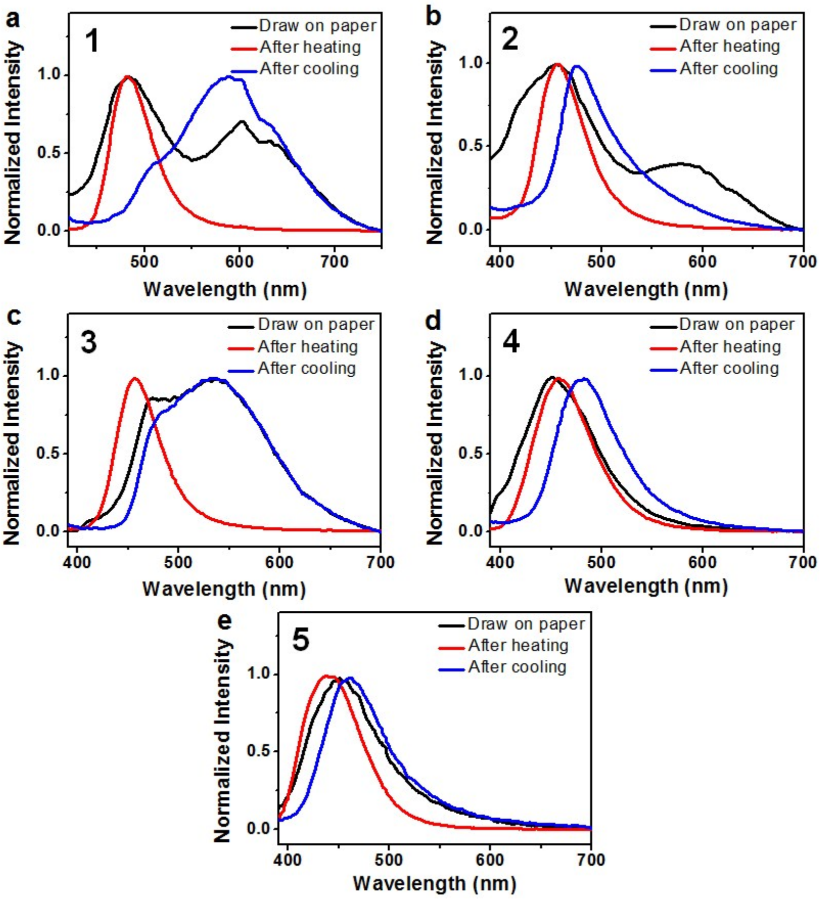

Fig. S29 (a–e) Fluorescence emission spectra of (**1** – **5**)-in-OA pen mechanical drawn content on filter paper and upon their first heating and cooling treatment.

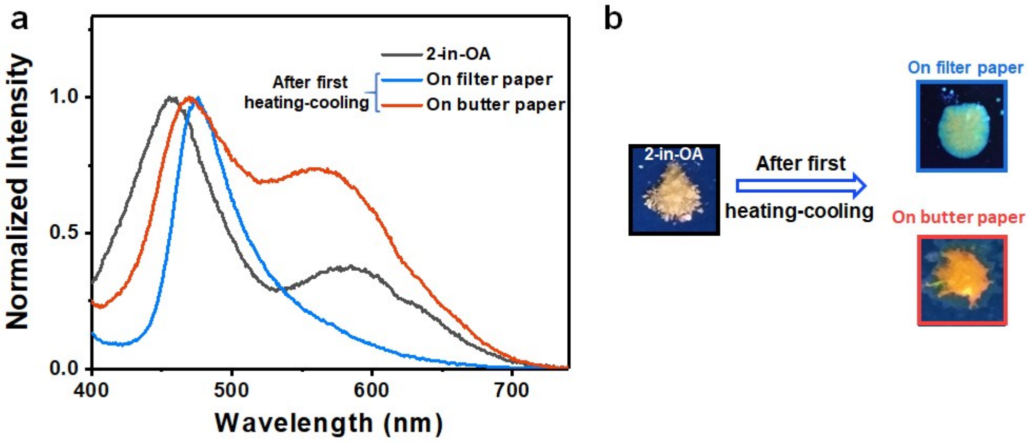

Fig. S30 (a) Fluorescence emission spectra of **2**-in-OA (black line) go through a heating-cooling treatment on filter paper (blue line) and butter paper (red line), respectively and (b) The corresponding photographs taken under 365 nm UV light.

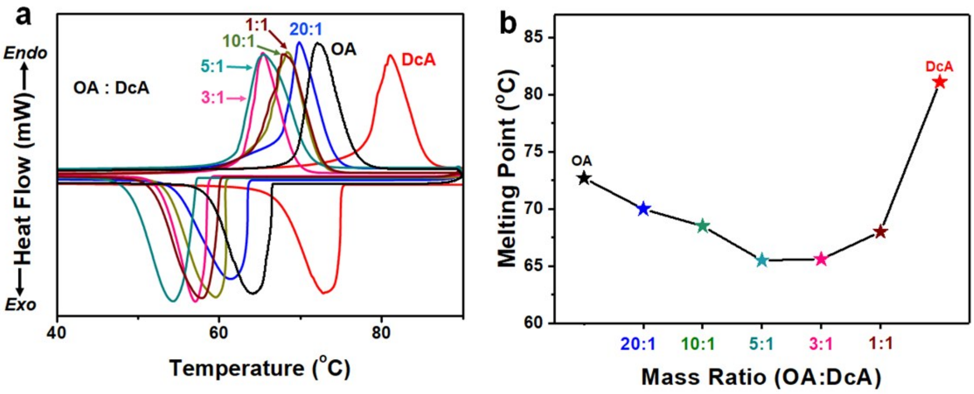

Fig. S31 (a) DSC thermograms of **3**-in-OA, **3**-in-DcA and different mixture mass ratio of both. (b) Plots of melting point dependence on different mixture mass ratio of **3**-in-OA and **3**-in-DcA. The mass ratio of **3** in FA are 0.3 wt%.

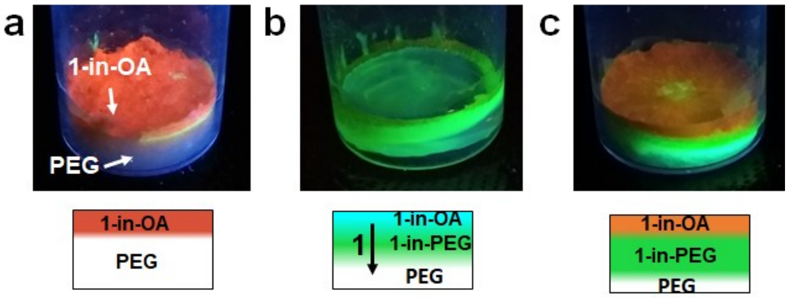

Fig. S32 Photographs (above) and diagrammatic sketch (below) of the process of coumarin **1** is extracted from OA to PEG after heating and cooling. (a) A layer of **1**-in-OA lay on the PEG layer, (b) during heating and (c) after cooling.

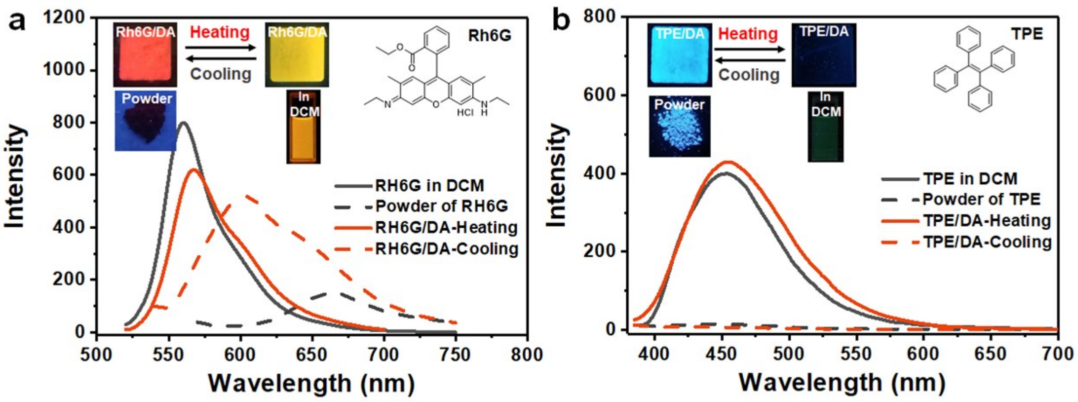

Fig. S33 (a) Fluorescence spectra and photographs of rhodamine 6G (Rh6G) in DA (0.056 wt%), on powder and in DCM (C = 1.0 × 10^{-4} mol L^{-1}). (RH6G in DCM: λ_{ex} = 500 nm, slit width (1.5, 1.5); Powder of RH6G: λ_{ex} = 550 nm, slit width (3, 5); RH6G/DA-Heating: λ_{ex} = 500 nm, slit width (3, 1.5); RH6G/DA-Cooling: λ_{ex} = 520 nm, slit width (3,5)) (b) Fluorescence spectra and photographs of tetraphenylethylene (TPE) in DA (0.1 wt%), on powder and in DCM (C = 1.0 × 10^{-4} mol L^{-1}). λ_{ex} = 365 nm, slit width (3, 1.5); Powder of TPE: slit width (1.5, 3).

Supplementary Discussions

Discussion S1.

To determine the optimum concentration of coumarin required to form an non-dispersion state, the experiment of gradually varying doping mass of **1**–**5** in DA have been tested, as shown in Fig. S13. Take **1**-in-DA as an example, in solid state, at a low concentration (*i.e.*, 0.1mg/g DA), the emission band around 503 nm is dominant. As the doping mass of **1** in per gram of DA increases, the emission intensity around 503 nm gradually decreases with the increase of emission intensity around 638 nm. When the doping mass reached 3 mg per gram of DA, the emission intensity around 503 nm decreased to the lowest point, and the emission intensity around 638 nm increased to the highest point and no longer increased, but fluctuates up and down as the doping mass continued to increase. For the convenience of observation, the relationship between maximum emission intensity and doping mass was performed as shown in Fig. S19. The 503 nm emission peak represents the dispersion state emission and the 638 nm emission peak represents the aggregation state emission. These data suggest that **1** is completely in the aggregation state in solid state when the doping mass reaches 3 mg in per gram of DA. In liquid state, the fluorescence intensity increases as the doping mass increases from 0.1 mg to 0.2 mg in per gram of DA. As the doping mass continues to increase, the fluorescence intensity gradually decrease, and the emssion peak gradually bathochromic shift. Comprehensive analysis the emission in solid and liquid state, the optimal doping mass for **1** in per gram DA is 3 mg. At this concentration, the coumarin can be completely in a state of aggregation and can maintain a relatively strong fluorescence emission.

2/**3**-in-DA have the same rules. It is worth noting that **2**-in-DA still has a dispersed state emission around 475 nm even if it reaches a supersaturated concentration. This phenomenon may be caused by the interreaction between **2** and DA beacuse they all have a -COOH group, and the interreaction causes the coumarin to not be well seperated from DA upon crystallization.

For **4**/**5**-in-DA, there are no obvious bathochromic shift in emission peak as the doping mass of **4**/**5** in per gram of DA increases. Under the consideration of the color contrast ratio and the high emission intensity, we choose a relative suitable concentration of 2mg/g DA for **4** and **5**, respectively.

Therefore, the optimal concentration for **1** – **5** are 3 mg, 1mg, 3 mg, 2 mg, 2 mg in per gram DA, respectively.

Discussion S2.

For **2**, there is only a red-shifted dispersed emission band was observed after its first cycle of heating-cooling treatment (Fig. S29b, blue line *vs.* black line). It's due to low solubility of **2** in OA (octadecanoic acid) (*e.g.*, less than 0.5 mg/g DA (dodecanoic acid)) and dispersion effect of the filter paper with porous structures. The latter was proved by the experiments that powder of **2**-in-OA shows blue emission and only a red-shifted dispersed emission band was observed on filter paper after a heating-cooling treatment (Fig. S30, blue line *vs.* black line). But it shows orange emission on butter paper with tight and dense structure and two broad emission bands especially with a great increase of emission intensity on the aggregation state around 586 nm were observed after a heating-cooling treatment (Fig. S30, red line *vs.* black line).

Supplementary Tables

Table S1 Fluorescence lifetime of **1** – **5** (0.3 wt%, 0.1 wt%, 0.3 wt%, 0.2 wt%, 0.2 wt%, respectively) dissolved in DA in solid and liquid states. λ_{ex} = 375 nm.

		τ_1[a] (ns)	**τ_2[a] (ns)**	**τ_3[a] (ns)**	**τ_{avg}[b] (ns)**	**χ^2 [c]**
1	s	3.05	7.39	20.29	7.84	1.329
	l	1.91	44.07	-	2.64	1.295
2	s	2.36	13.33	32.16	30.04	1.226
	l	2.32	6.37	-	2.49	1.309
3	s	1.62	5.29	14.50	10.84	1.217
	l	2.40	8.76	-	2.58	1.341
4	s	0.71	2.49	-	1.50	1.801
	l	3.49	9.72	-	3.62	1.187
5	s	0.61	2.84	-	1.35	1.736
	l	3.52	-	-	3.52	1.391

[a] Fluorescence lifetime;

[b] Average lifetime;

[c] Goodness of fit.

Table S2 Fluorescence lifetime of **4** on powder and crystal state. λ_{ex} = 375 nm.

	τ_1[a] (ns)	τ_2[a] (ns)	τ_{avg}[b] (ns)	χ^2[c]
Powder	0.74	2.68	1.10	1.628
Crystal	0.80	3.39	1.80	1.626

[a] Fluorescence lifetime;

[b] Average lifetime;

[c] Goodness of fit.

Table S3 Thermal properties, crystallinity of PEG, PCL

Sample	**T_m[a] (^oC)**	**ΔH_m[b] (J/g)**	**ΔH^0_m[c] (J/g)**	**Crystallinity[d] (%)**
PEG	67.45	166.6	219.34	75.9
PCL	57.04	58.30	135.62	42.9

[a] Melting point;

[b] Heat of fusion of measured at T_m;

[c] Reference values of heat fusion for 100% crystalline; [5, 6]

[d] Calculated by equation ($\Delta H_m/\Delta H^0_m$).

References

1 W. Y. Kim, H. Shi, H. S. Jung, D. Cho, P. Verwilst, J. Y. Lee, J. S. Kim, *Chem. Commun.* 2016, **52**, 8675.

2 K. Huang, M. Liu, X. Wang, D. Cao, F. Gao, K. Zhou, W. Wang, W. Zeng, *Tetrahedron Lett.* 2015, **56**, 3769.

3 M. Liu, M. Hu, Q. Jiang, Z. Lu, Y. Huang, Y. Tan, Q. Jiang, *RSC Adv.* 2015, **5**, 15778.

4 P. W. Winston, D. H. Bates, *Ecology* 1960, **41**, 232.

5 S. S. Kim, Y. M. Lee, C. S. Cho, *J. Polym. Sci., Part A: Polym. Chem.* 1995, **36**, 4497.

6 F. Li, J. Hou, W. Zhu, X. Zhang, M. Xu, X. Luo, D. Ma, B. K. Kim, *J. Appl. Polym. Sci.* 1996, **62**, 631.